J|A|C|S
ARTICLES
Published on Web 06/25/2003

Cyclic Polyamidato Dianions as Bridges between Mo_2^{4+} Units: Synthesis, Crystal Structures, Electrochemistry, Absorption Spectra, and Electronic Structures

F. A. Cotton,*,† James P. Donahue,† Carlos A. Murillo,*,† Lisa M. Pérez,‡ and Rongmin Yu†

Contribution from the Laboratory for Molecular Structure and Bonding, Department of Chemistry, Texas A&M University, College Station, Texas 77842-3012 and Laboratory for Molecular Simulation, Department of Chemistry, Texas A&M University, College Station, Texas 77842-3012

Received April 25, 2003; E-mail: cotton@tamu.edu; murillo@tamu.edu

Abstract: Compounds in which quadruply bonded Mo_2^{4+} units, $Mo_2(DAniF)_3$ (DAniF = *N,N′*-di-*p*-anisylformamidinate), are linked by cyclic diamidate anions have been synthesized and characterized by X-ray crystallography and spectroscopic methods. As identified by the diamidate linker, these compounds are 4,6-dioxypyrimidinate (**2**), 2,3-dioxypyrazinate (**3**), 2,3-dioxyquinoxalinate (**4**), 2,3-dioxy-5,6-dicyanopyrazinate (**5**), and cyanurate (**6**). With uracilate, a dinuclear unlinked 1:1 adduct is formed, $Mo_2(DAniF)_3$-(uracilate) (**1**). The cyclic voltammograms of **3**−**5** reveal significantly larger $\Delta E_{1/2}$ values (258 mV−308 mV) than that of the oxalate linked analogue (212 mV), which is indicative of greater charge delocalization in the mixed valent Mo_2^{4+}/Mo_2^{5+} species and hence greater communication between the two Mo_2 units. $\Delta E_{1/2}$ for **2** is substantially lower than those for **3**−**5**. This difference is attributed to the *meta* disposition of the two amidate groups in 4,6-dioxypyrimidinate as compared to their *ortho* arrangement in the pyrazinate-type linkers. The absorption spectra of the linked compounds **3**−**5** are more complex than those of the analogous polyunsaturated dicarboxylate linked compounds and reveal at least two significant absorption bands within the region 420−550 nm. Compound **2** also has two bands but with significantly lower intensity. Time dependent DFT calculations upon **2** and **3** indicate rather different electronic structures for these two structural isomers. The two bands for **3** have $\delta \rightarrow \pi^*$ character, and the π^* type orbitals have substantial contributions from the Mo_2 units as well as from the diamidate linker. The excitations observed in **2** are mainly metal based. The differences between the electronic spectra of **2** and **3** are consistent with the electrochemistry in underscoring the profound physical effect of changing the symmetry of the diamidate linker.

Introduction

The relative effectiveness of various groups that may link structurally two metal atoms, or groups of metal atoms, in communicating electronic changes from one metal atom(s) to the other(s) is clearly a fundamental question in chemistry. With respect to molecules with a single metal atom at each end, enormous effort and ingenuity have already gone into answering it, and a great deal of progress has been made.[1] The very next larger entity after a single metal atom is, obviously, a pair of metal atoms. In this realm, there is still much that we do not know. The earliest serious effort to link pairs of dimetal units was published in 1991 by Chisholm et al.,[2] who studied solution properties of molecules of type Ia (Scheme 1). Unfortunately, to this day these molecules have, apparently, defied all efforts to isolate them in a form suitable for standard X-ray crystallographic characterization, although Chisholm has carried out other pertinent studies.[3]

In 1998, the isolation and structural characterization of molecules of type I, namely those in Ib, were reported.[4] More detailed, structurally complete studies of many Ib molecules with a highly varied array of X units have appeared more recently,[5] and many more complex but related structures (e.g., squares, triangles, and loops) have also been prepared, crystallographically defined, and studied in other ways.[6] In nearly all

† Laboratory for Molecular Structure and Bonding.
‡ Laboratory for Molecular Simulation.

(1) For example, see: (a) Creutz, C. *Prog. Inorg. Chem.* **1983**, *30*, 1. (b) Chen, P.; Meyer, T. J. *Chem. Rev.* **1998**, *98*, 1439. (c) Ferretti, A.; Lami, A.; Murga, L. F.; Shehadi, I. A.; Ondrechen, M. J.; Villani, G. *J. Am. Chem. Soc.* **1999**, *121*, 2594. (d) Kaim, W.; Klein, A.; Gloeckle, M. *Acc. Chem. Res.* **2000**, *33*, 755. (e) Demadis, K. D.; Hartshorn, C. M.; Meyer, T. J. *Chem. Rev.* **2001**, *101*, 2655. (f) Brunschwig, B. S.; Creutz, C.; Sutin, N. *Chem. Soc. Rev.* **2002**, *31*, 168. (g) Lau, V. C.; Berben, L. A.; Long, J. R. *J. Am. Chem. Soc.* **2002**, *124*, 9042.
(2) Cayton, R. H.; Chisholm, M. H.; Huffman, J. C.; Lobkovsky, E. B. *J. Am. Chem. Soc.* **1991**, *113*, 8709.
(3) (a) Bursten, B. E.; Chisholm, M. H.; Hadad, C. M.; Li, J.; Wilson, P. J. *Chem. Commun.* **2001**, 2382. (b) Bursten, B. E.; Chisholm, M. H.; Clark, R. J. H.; Firth, S.; Hadad, C. M.; MacIntosh, A. M.; Wilson, P. J.; Woodward, P. M.; Zaleski, J. M. *J. Am. Chem. Soc.* **2002**, *124*, 3050. (c) Bursten, B. E.; Chisholm, M. H.; Clark, R. J. H.; Firth, S.; Hadad, C. M.; Wilson, P. J.; Woodward, P. M.; Zaleski, J. M. *J. Am. Chem. Soc.* **2002**, *124*, 12244.
(4) Cotton, F. A.; Lin, C.; Murillo, C. A. *J. Chem. Soc., Dalton Trans.* **1998**, 3151.

10.1021/ja0358044 CCC: $25.00 © 2003 American Chemical Society

Scheme 1. Dicarboxylate Linked $M_2(O_2CR)_3^+$ (**Ia**) and $M_2(ArNC(H)NAr)_3^+$ (**Ib**) Units

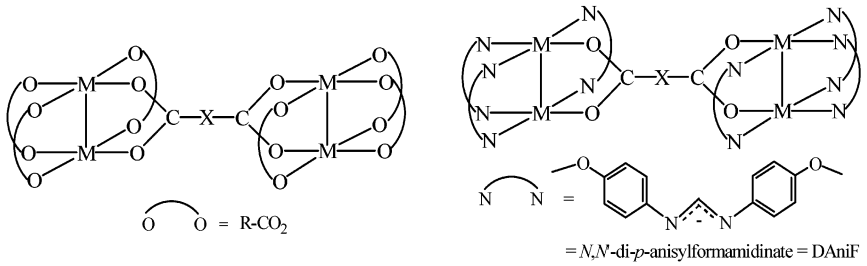

Ia **Ib**

Scheme 2. Structures of Diamidate (**IIa**) and Diamidinate (**IIb**) Linkers

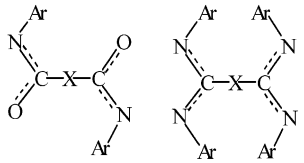

IIa **IIb**

of the compounds alluded to so far, the linkers have been dicarboxylic acids. The question naturally arose as to whether diamidates (IIa) and diamidinates (IIb) (Scheme 2) would be more efficient than carboxylates in effecting electronic coupling between dimetal units. One report has appeared describing the deliberate synthesis, structures, and other properties of two such compounds.[7] In this work, two straightforward examples of type IIa diamidates were used.

We have recognized that there is a special class of diamidates that have no dicarboxylate analogues and that these could give rise to coupling between dimetal units that might exceed that which can be achieved in other ways. The precursors of the entire set of five isomeric cyclic diamidate ligands (or potential ligands) are depicted in Scheme 3(IIIa); for simplicity all are shown in the same extreme tautomeric form. Our primary goal in this work was to see how much synthetic chemistry could be accomplished by employing these as linkers between two $(DAniF)_3Mo_2^+$ units and measuring electrochemically how effective they are in mediating electronic communication. Scheme 3 (IIIb), analogously, shows two similar compounds that have also been used as linkers. Among those in Scheme 3 (IIIa), only two of the five, B and C, have been incorporated into the type of product we were seeking. Uracil, A, could not be incorporated into this type of structure for steric reasons, but a 1:1 adduct with $(DAniF)_3Mo_2^+$ has been made. There can be little doubt that E would also be incapable, for steric reasons, of serving as a linker (a point to be discussed later). The precursor of the potential linker D is poorly characterized and difficult to synthesize without sterically unencumbering substituents,[8] and we have not undertaken to use it.

Thus, we report a total of six compounds here in which linkers B, C, F, G, and H as well as the ligand A have been used. For all six, we report the crystal structures and their electrochemistry. From the pair of oxidation potentials in each of the five linked molecules, we infer the abilities of the linkers to delocalize charge over both dimetal units when only one has been oxidized.

In all the compounds mentioned above, the communication between the dimetal centers has been studied by electrochemistry. The effectiveness of communication has been assessed in terms of $\Delta E_{1/2}$, the difference between the first and second oxidation potentials.[9] These have ranged from <100 mV to a high of 225 mV for dicarboxylate-linked molecules of type Ib. Still higher values were found when the $O_2CXCO_2^{2-}$ linkers were replaced by EO_4^{2-} ions, E = S, Mo, and W.[10]

In the work reported here, we have sought the answers to two main questions: (1) Can molecules of type IIa be made in which the diamidate bridge is a cyclic polyamidate (or a tautomer thereof)? (2) How effective will cyclic polyamidate linkers be in mediating communication between the two dimetal units? In planning this research, we considered all the precursors to the dianionic linkers shown in Scheme 3 (IIIa). Practical considerations (e.g., commercial availability, accessibility via synthesis, probability of adding significantly to our understanding in return for the additional work required) limited our choice to those reported here.

It should be noted that some of the ligand precursors have important roles in biological processes, and an enormous amount of literature has been dedicated to a few of them. For example, cyanuric acid and uracil, which have a close structural relationship, have been often studied for their ability to form hydrogen bonds in structures that vary from simple pairs to extended supramolecular networks.[11] Much of this work has been based on the concept of base pair recognition that mimics the pairing of adenine (A) with thymine (T) and guanine (G) with cytosine (C) by hydrogen bond formation that is so important in the formation of the DNA double helix.[12] However, the amount of literature on the interaction of this type of compound with transition metal atoms (which are abundant in enzymes) is very limited.

Experimental Section

Materials and Methods. All manipulations and procedures were conducted under N_2 using either an N_2 drybox or standard Schlenk line techniques. Solvents were distilled and/or degassed immediately

(5) (a) Cotton, F. A.; Donahue, J. P.; Lin, C.; Murillo, C. A. *Inorg. Chem.* **2001**, *40*, 1234. (b) Cotton, F. A.; Donahue, J. P.; Murillo, C. A. *Inorg. Chem. Commun.* **2002**, *5*, 59. (c) Cotton, F. A.; Donahue, J. P.; Murillo, C. A. *J. Am. Chem. Soc.* **2003**, *125*, 5436.
(6) (a) Cotton, F. A.; Lin, C.; Murillo, C. A. *Acc. Chem. Res.* **2001**, *34*, 759. (b) Cotton, F. A.; Lin, C.; Murillo, C. A. *Proc. Nat. Acad. Sci., U.S.A.* **2002**, *99*, 4810.
(7) Cotton, F. A.; Daniels, L. M.; Donahue, J. P.; Liu, C. Y.; Murillo, C. A. *Inorg. Chem.* **2002**, *41*, 1354.
(8) Adachi, J.; Sato, N. *J. Heterocyclic Chem.* **1986**, *23*, 871.
(9) Richardson, D. E.; Taube, H. *Inorg. Chem.* **1981**, *20*, 1278.
(10) Cotton, F. A.; Donahue, J. P.; Murillo, C. A. *Inorg. Chem.* **2001**, *40*, 2229.
(11) For example, see: (a) MacDonald, J. C.; Whitesides, G. M. *Chem. Rev.* **1994**, *94*, 2383. (b) Pedireddi, V. R.; Ranganathan, A.; Ganesh, K. N. *Org. Lett.* **2001**, *3*, 99. (c) Prins, L. J.; Hulst, R.; Timmerman, P.; Reinhoudt, D. N. *Chem.—Eur. J.* **2002**, *8*, 2288. (d) Falvello, L. R.; Garde, R.; Tomás, M. *Inorg. Chem.* **2002**, *41*, 4599.
(12) (a)Watson, J. D.; Crick, F. H. C. *Nature* **1953**, *171*, 737. (b) Saenger, W. *Principles of Nucleic Acid Structure*; Springer-Verlag: New York, 1984. (c) Neidle, S. *Nucleic Acid Structure and Recognition*; Oxford University Press: Oxford, 2002.

Scheme 3. Five Monocyclic Diamide Ligands (**IIIa**)[a]

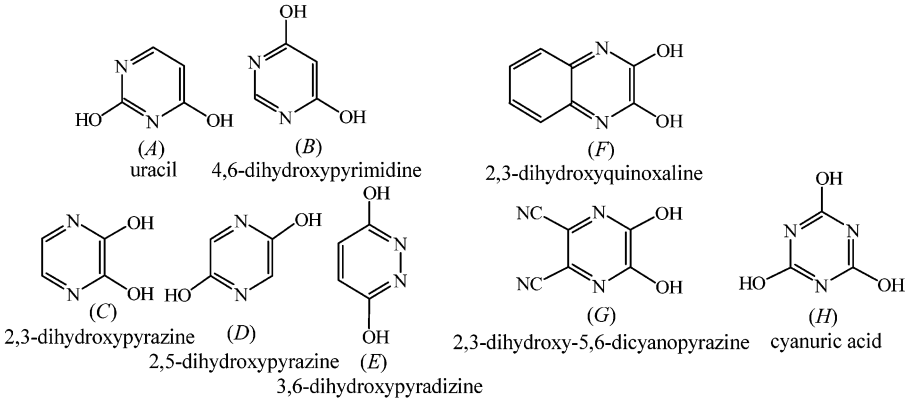

[a] For convenience, these linking ligands are all written in the hydroxyamine tautomeric form. Other available cyclic diamide ligands (**IIIb**) are also shown as well as the potentially trischelating ligand cyanuric acid (**IIIc**). [b]These distances are between the Mo atoms and the N or O atoms of the linker.

prior to use; MeCN was twice distilled under N_2, first from activated molecular sieves and then from CaH_2, CH_2Cl_2 was dried and distilled from P_2O_5, and THF, Et_2O, and hexanes were distilled from Na/K-benzophenone. Chlorobenzene was not distilled but dried by filtration through anhydrous Na_2SO_4 and degassed with vigorous N_2 bubbling immediately prior to use. $Mo_2(DAniF)_3Cl_2$[13] and 2,3-dihydroxypyrazine[14] were prepared by literature methods, and all tetraethylammonium salts of the polyamidate compounds were prepared and isolated as solids by neutralizing the corresponding diamide compound with 2 equiv of Et_4NOH followed by carefully drying under vacuum.

Physical Methods. Elemental analyses were performed by Canadian Microanalytical Service, Delta, British Columbia, upon crystalline samples that were dried overnight under vacuum. Where the presence of residual solvent was indicated by ^1H NMR spectroscopy, it was factored into the expected elemental analysis. ^1H NMR spectra were recorded on a Varian XL-200AA NMR spectrometer with chemical shifts referenced to the protonated solvent residual. Absorption spectra were measured at room temperature under N_2 using a Shimadzu UV-2501 PC spectrophotometer. The cyclic voltammograms and differential pulse voltmmograms were taken with a CH Instruments model-CH1620A electrochemical analyzer in 0.1 M Bu_4NPF_6 solution in CH_2Cl_2 with Pt working and auxiliary electrodes, an Ag/AgCl reference electrode, and a scan rate of 100 mV/s. All the potential values are referenced to the Ag/AgCl electrode, and under the present experimental conditions, the $E_{1/2}$ (Fc^+/Fc) consistently occurred at +440 mV in CH_2Cl_2 and at +574 mV in THF.

X-ray Structure Determinations. The six molybdenum compounds prepared from ligands A−C and F−H are indicated with numbers in bold-faced type as **1**−**3** and **4**−**6**, respectively. Single crystals suitable for X-ray diffraction analysis were grown by diffusion of Et_2O (**1**, **3**−**5**) or hexanes (**2**) into a CH_2Cl_2 solution of the corresponding product. Crystals of **6**·C_6H_5Cl·Et_2O were obtained by slow diffusion of a 1:10 Et_2O:hexanes mixture into a saturated C_6H_5Cl solution. Single-crystal X-ray work on $[Mo_2(DAniF)_3]_2$(μ-4,6-dioxypyrimidinate) (**2**) was performed on a Nonius Fast diffractometer utilizing the program MADNES.[15] A suitable crystal was mounted on the tip of a quartz fiber with a small amount of silicone grease and transferred to a goniometer head. Cell parameters were obtained from an autoindexing routine and were refined with 250 reflections within a 2θ range 18.1−41.6°. Cell dimensions and Laue symmetry for the crystals were confirmed with axial photographs. All data were corrected for Lorentz and polarization effects. Data were processed using an ellipsoid-mask algorithm (the program PROCOR[16]), and the program SORTAV[17] was used to correct for absorption. Data for $[Mo_2(DAniF)_3(uracilate)]$·$CH_2Cl_2$·$C_6H_{14}$ (**1**·CH_2Cl_2·C_6H_{14}), $[Mo_2(DAniF)_3]_2$(μ-2,3-dioxypyrazinate)·$4CH_2Cl_2$ (**3**·$4CH_2Cl_2$), $[Mo_2(DAniF)_3]_2$(μ-2,3-dioxyquinoxalinate)·$3CH_2Cl_2$ (**4**·$3CH_2Cl_2$), $[Mo_2(DAniF)_3]_2$(μ-2,3-dicyano-5,6-dioxypyrazinate)·$2CH_2Cl_2$·Et_2O (**5**·$2CH_2Cl_2$·Et_2O), and $[Mo_2(DAniF)_3]_2$(μ-cyanurate)·C_6H_5Cl·Et_2O (**6**·C_6H_5Cl·Et_2O) were collected using a Bruker SMART 1000 CCD area detector system using ω scans. The first 50 frames were recollected at the end of the data collection to monitor for crystal decay, but no significant decomposition was observed. Cell parameters were determined using the program SMART.[18] Data reduction and integration were performed with the software package SAINT,[19] which corrects for Lorentz and polarization effects, while absorption corrections were applied by using the program SADABS.[19]

In all structures, the positions of the Mo atoms were found via direct methods using the SHELXL software.[20] The positions of the remaining non-hydrogen atoms were revealed by subsequent cycles of least-squares refinements followed by difference Fourier syntheses. All hydrogen atoms, except H(8A) in **1** and H(15) in **6**, were added in calculated positions and refined isotropically as riding atoms with displacement parameter values equal to 1.2 times those of the carbon atoms to which they are attached. Cell parameters and refinement results for all compounds are summarized in Table 1, while key metric parameters are collected in Tables 2 and 3.

Computational Details. All calculations were performed with the Gaussian 98 (G98) suite of programs[21] using a double-ζ basis set (D95) on the C, N, O, and H atoms.[22] A small (1s2s3s2p3p3d) effective core potential (ECP) was used for the Mo atoms with a double-ζ quality basis set.[23] To investigate the electronic structure of compounds **2** and

(13) Cotton, F. A.; Daniels, L. M.; Jordan, G. T., IV; Lin, C.; Murillo, C. A. *J. Am. Chem. Soc.* **1998**, *120*, 3398.
(14) Adachi, J.; Sato, N. *J. Org. Chem.* **1972**, *37*, 221.
(15) Pflugrath, J. W.; Messerschmidt, A. *MADNES, Munich Area Detector (New ECC) System*, version EEC 11/1/89, with enhancements by Nonius Corporation, Delft, The Netherlands. A description of MADNES appears in the following: Messerschmidt, A.; Pflugrath, J. W. *J. Appl. Crystallogr.* **1987**, *20*, 306.
(16) (a) Kabsch, W. *J. Appl. Crystallogr.* **1988**, *21*, 67. (b) Kabsch, W. *J. Appl. Crystallogr.* **1988**, *21*, 916.
(17) Blessing, R. H. *Acta Crystallogr.* **1995**, *A51*, 33.
(18) *SMART for Windows NT*, version 5.618; Bruker Analytical X-ray Systems: 2000.
(19) *SAINT+ for NT*, Version 6.28A.; Bruker Analytical X-ray Systems: 2001.
(20) Sheldrick, G. M. *SHELX-97 Programs for Crystal Structure Analysis*. Institüt fürAnorganische Chemie der Universität: Tammanstrasse 4, D-3400, Göttingen, Germany, 1998.
(21) Frisch, M. J.; Trucks, G. W.; Schlegel, H. B.; Scuseria, G. E.; Robb, M. A.; Cheeseman, J. R.; Zakrzewski, V. G.; Montgomery, J. A.; Stratmann, R. E.; Burant, J. C.; Dapprich, S.; Millam, J. M.; Daniels, A. D.; Kudin, K. N.; Strain, M. C.; Farkas, O.; Tomasi, J.; Barone, V.; Cossi, M.; Cammi, R.; Mennucci, B.; Pomelli, C.; Adamo, C.; Clifford, S.; Ochterski, J.; Petersson, G. A.; Ayala, P. Y.; Cui, Q.; Morokuma, K.; Malick, D. K.; Rabuck, A. D.; Raghavachari, K.; Foresman, J. B.; Cioslowski, J.; Ortiz, J. V.; Stefanov, B. B.; Liu, G.; Liashenko, A.; Piskorz, P.; Komaromi, I.; Gomperts, R.; Martin, R. L.; Fox, D. J.; Keith, T.; Al-Laham, M. A.; Peng,

Table 1. Crystallographic Data for the Linked Compounds $[Mo_2(DAniF)_3]_2(OCN-X-NCO)$ and for **1**·CH_2Cl_2·C_6H_{14}

compound	**1**·CH_2Cl_2·C_6H_{14}	**2**	**3**·$4CH_2Cl_2$	**4**·$3CH_2Cl_2$	**5**·$2CH_2Cl_2$·Et_2O	**6**·C_6H_5Cl·Et_2O
formula	$C_{56}H_{64}Cl_2Mo_2N_8O_8$	$C_{94}H_{92}Mo_4N_{14}O_{14}$	$C_{98}H_{100}Cl_8Mo_4N_{14}O_{14}$	$C_{101}H_{100}Cl_6Mo_4N_{14}O_{14}$	$C_{102}H_{104}Cl_4Mo_4N_{16}O_{15}$	$C_{103}H_{106}ClMo_4N_{15}O_{16}$
fw, g mol^{-1}	1239.93	2025.58	2365.28	2330.41	2319.57	2229.24
crystal system	triclinic	monoclinic	triclinic	triclinic	monoclinic	monoclinic
space group	$P\bar{1}$	$P2_1/n$	$P\bar{1}$	$P\bar{1}$	$P2/c$	$C2/c$
a (Å)	11.0140(8)	10.613(2)	12.467(1)	12.5325(8)	16.581(3)	30.021(2)
b (Å)	15.354(1)	24.806(4)	14.620(2)	14.3280(9)	17.679(3)	11.8606(9)
c (Å)	17.810(1)	33.840(2)	15.275(2)	15.380(1)	18.365(3)	56.867(4)
α (deg)	64.940(1)	90	71.936(2)	72.668(1)	90	90
β (deg)	87.207(1)	90.72(1)	83.479(2)	84.678(1)	110.131(3)	94.857(1)
γ (deg)	86.798(1)	90	71.188(2)	72.656(1)	90	90
V (Å^3)	2723.1(3)	8909(2)	2505.3(5)	2516.4(3)	5055(2)	20176(3)
Z	2	4	1	1	2	8
d_{calc} (g cm^{-3})	1.512	1.510	1.568	1.538	1.524	1.468
μ (mm^{-1})	0.621	0.623	0.722	0.716	0.663	0.585
2θ range (deg)	4.4−55.0	4.0−45.1	3.5−45.1	4.2−50.1	3.3−45.1	3.2−45.1
λ, Å	0.710 73	0.710 73	0.710 73	0.710 73	0.710 73	0.710 73
T, °C	−60	−60	−60	−60	−60	−60
goodness-of-fit	1.041	1.102	1.041	1.079	1.142	1.088
R1[a], wR2[b] ($I > 2\sigma(I)$)	0.046, 0.120	0.052, 0.118	0.054, 0.144	0.054, 0.139	0.067, 0.155	0.073, 0.154

[a] $R1 = \sum||F_o| - |F_c||/\sum|F_o|$. [b] $wR2 = [\sum[w(F_o^2 - F_c^2)^2]/w(F_0^2)^2]^{1/2}$, $w = 1/[\sigma^2(F_o^2) + (aP)^2 + bP]$, where $P = [\max(F_o^2 \text{ or } 0) + 2(F_c^2)]/3$.

Table 2. Selected Interatomic Distances for Compounds **1**−**6**

	1	**2**	**3**	**4**	**5**	**6**
d,[a] Å		7.256	7.081	7.089	7.128	7.318
Mo(1)−Mo(2)	2.0938(4)	2.0893(8)	2.0917(7)	2.0904(6)	2.095(1)	2.097(1)
Mo(3)−Mo(4)		2.0844(8)				2.096(1)
Mo−O[b]	2.128(3)	2.099(4)	2.153(4)	2.21(1)	2.145(5)	2.136(5)
		2.121(4)				2.128(5)
Mo−N[b]	2.200(3)	2.229(5)	2.148(4)	2.16(1)	2.192(5)	2.245(6)
		2.212(5)				2.247(6)
Mo(1)−N(1)	2.169(3)	2.131(5)	2.161(5)	2.171(4)	2.178(6)	2.147(7)
Mo(1)−N(3)	2.120(3)	2.151(5)	2.131(5)	2.126(4)	2.138(6)	2.126(6)
Mo(1)−N(5)	2.182(3)	2.137(5)	2.159(5)	2.166(4)	2.170(6)	2.144(8)
Mo(2)−N(2)	2.144(3)	2.174(5)	2.122(5)	2.136(4)	2.120(7)	2.145(7)
Mo(2)−N(4)	2.127(3)	2.131(5)	2.147(5)	2.144(4)	2.133(6)	2.124(7)
Mo(2)−N(6)	2.126(3)	2.149(5)	2.142(5)	2.148(4)	2.130(7)	2.136(8)
Mo(3)−N(7)		2.137(6)				2.163(8)
Mo(3)−N(9)		2.101(5)				2.120(7)
Mo(3)−N(11)		2.142(5)				2.133(8)
Mo(4)−N(8)		2.155(6)				2.153(7)
Mo(4)−N(10)		2.132(5)				2.131(7)
Mo(4)−N(12)		2.120(5)				2.158(8)
selected bond distances for linkers	O(7)−C(48)	O(1)−C(1)	O(7)−C(47)	O(7)−C(1)	O(7)−C(46)	O(15)−C(3)
	1.277(4)	1.292(7)	1.326(7)	1.296(6)	1.278(8)	1.211(9)
	O(8)−C(49)	O(2)−C(2)	N(7)−C(47)	N(7)−C(1)	N(7)−C(46)	O(13)−C(1)
	1.249(5)	1.288(7)	1.318(7)	1.368(6)	1.346(9)	1.280(9)
	N(7)−C(48)	C(1)−N(13)	N(7)−C(48)	C(1)−C(1A)	N(7)−C(47)	O(14)−C(2)
	1.365(5)	1.395(8)	1.38(1)	1.459(8)	1.387(9)	1.277(9)
	N(7)−C(49)	C(2)−N(14)	C(47)−C(47A)	N(7)−C(7A)	N(8)−C(48)	N(13)−C(1)
	1.366(5)	1.395(9)	1.45(1)	1.45(2)	1.15(1)	1.32(1)

[a] d = distance between centroids of the two Mo_2 units. [b] Distances to linker N and O atoms.

3, single point energy calculations[24] were performed using density functional theory (DFT)[25] with the Becke three parameter hybrid exchange functional[26] and the Lee−Yang−Parr correlation functional (B3LYP).[27] For feasibility purposes, the calculations were simplified by replacing each *p*-anisyl substituent with a hydrogen atom. To gain insight into the electronic transitions responsible for the observed UV−vis spectra of **2** and **3**, time-dependent density functional theory[28] (TDDFT) calculations were performed on Origin 2000 and Origin 3800 computers at the Texas A&M University Supercomputing facility and on an SGI Power Challenge in the Department of Chemistry, Texas A&M University.

Preparation of Compounds. The procedure used was that of method B in ref 5a.

$Mo_2(DAniF)_3$(uracilate) (1). Tetraethylammonium uracilate was used in the stoichiometric ratio of 1:1 with $Mo_2(DAniF)_3Cl_2$. Yield: yellow prisms, 40%. ^{1}H NMR (ppm in CD_2Cl_2): 10.23 (br, s, 1H, N−*H*), 8.52 (s, 2H, −NC*H*N−), 8.42 (s, 1H, aromatic C−H), 6.98 (m, 2H, aromatic C−H), 6.38−6.74 (m, 20H, aromatic C−H), 6.10−6.24 (m, 4H, aromatic C−H), 3.71 (s, 6H, −OCH_3), 3.65 (s, 6H, −OCH_3), 3.64 (s, 18H, −OCH_3). Absorption spectrum (CH_2Cl_2) λ_{max} (ϵ_M): 257 (48 700), 297 (50 200), 405 (7230), 460 (3880). Anal. Calcd for $C_{49}H_{48}Mo_2N_8O_8$: C, 55.06; H, 4.53; N, 10.48. Found: C, 54.75; H, 4.45; N, 10.38%.

$[Mo_2(DAniF)_3]_2$(μ-4,6-dioxypyrimidinate) (2). Yield: orange plates, 40%. ^{1}H NMR (δ in CD_2Cl_2): 8.58 (s, 4H, −NC*H*N−), 8.30 (s, 1H, pyrimidinate C−H), 8.25 (s, 2H, −NC*H*N−), 6.59−6.70 (m, 16H,

C. Y.; Nanayakkara, A.; Gonzalez, C.; Challacombe, M.; Gill, P. M. W.; Johnson, B. G.; Chen, W.; Wong, M. W.; Andres, J. L.; Head-Gordon, M.; Replogle, E. S.; Pople, J. A. Gaussian 98, revision A.6, A.7, and A.9; Gaussian, Inc.: Pittsburgh, PA 1998.
(22) Dunning, T. H.; Hay, P. J. In *Methods of Electronic Structure Theory*, Vol. 3; Schaefer, H. F., III, Ed.; Plenum Press: New York, 1977.
(23) Hay, P. J.; Wadt, W. R. *J. Chem. Phys.* **1985**, *82*, 299.
(24) The convergence criterion for the SCF was increased from a default value of 10^{-4} to 10^{-8}.
(25) Parr, R. G.; Yang, W. *Density-Functional Theory of Atoms and Molecules*; Oxford University Press: Oxford, 1989.
(26) (a) Becke, A. D. *Phys. Rev. A.* **1998**, *38*, 3098. (b) Becke, A. D. *J. Chem. Phys.* **1993**, *98*, 1372. (c) Becke, A. D. *J. Chem. Phys.* **1993**, *98*, 5648.
(27) Lee, C. T.; Yang, W. T.; Parr, R. G. *Phys. Rev. B* **1998**, *37*, 785.
(28) Casida, M. E.; Jaorski, C.; Casida, K. C.; Salahub, D. R. *J. Chem. Phys.* **1998**, *108*, 4439.

Table 3. Selected Angles for Compounds **1**−**6**

	1	2	3	4	5	6
Φ,[a] deg		35.9	0	0	5.1	3.2
X(1)−Mo(1)−N(1)[b]	90.9(1)	85.9(2)	87.7(2)	92.1(3)	91.9(2)	83.8(2)
X(1)−Mo(1)−N(3)[b]	177.7(1)	170.2(2)	174.5(2)	172.7(2)	176.6(2)	171.3(3)
X(1)−Mo(1)−N(5)[b]	90.4(1)	88.9(2)	87.4(2)	84.4(3)	88.1(2)	88.3(2)
X(2)−Mo(2)−N(2)[b]	87.3(1)	92.5(2)	86.1(2)	84.4(3)	89.1(2)	88.4(2)
X(2)−Mo(2)−N(4)[b]	171.6(1)	176.8(2)	174.5(2)	173.7(3)	173.0(2)	177.7(3)
X(2)−Mo(2)−N(6)[b]	89.4(1)	85.5(2)	89.6(2)	92.2(3)	90.3(2)	92.1(3)
X(3)−Mo(3)−N(7)		85.8(2)				85.5(3)
X(3)−Mo(3)−N(9)		171.6(2)				170.8(2)
X(3)−Mo(3)−N(11)		90.1(2)				88.1(2)
X(4)−Mo(4)−N(8)		91.3(2)				88.8(2)
X(4)−Mo(4)−N(10)		176.1(2)				177.5(3)
X(4)−Mo(4)−N(12)		84.7(2)				92.6(2)
N(1)−Mo(1)−N(5)	175.4(1)	172.9(2)	173.4(2)	174.3(1)	175.2(2)	170.9(3)
N(2)−Mo(2)−N(6)	173.1(1)	174.0(2)	172.9(2)	173.1(1)	173.6(3)	174.8(3)
N(7)−Mo(3)−N(11)		174.1(2)				172.5(3)
N(8)−Mo(4)−N(12)		172.9(2)				173.9(3)
selected bond angles for linker	C(48)−N(7)−C(49) 120.1(3)	O(1)−C(1)−N(13) 116.6(5)	O(7)−C(47)−N(7) 119.3(5)	O(7)−C(1)−N(7) 122.5(8)	O(7)−C(46)−N(7) 119.2(6)	O(1)−C(1)−N(13) 122.9(7)
	O(7)−C(48)−N(7) 118.2(3)	O(2)−C(2)−N(14) 117.6(6)	C(47)−N(7)−C(48) 116.9(7)	C(1)−N(7)−C(7A) 124(1)	C(46)−N(7)−C(47) 116.3(6)	O(2)−C(2)-N(14) 122.6(7)
	O(8)−C(49)−N(7) 120.8(3)	N(13)−C(3)−N(14) 127.9(6)	N(7)−C(7)−C(47A) 121.0(7)	O(7)−C(1)−C(1A) 118.4(7)	N(7)−C(46)−C(46A) 120.7(4)	N(13)−C(3)−O(3) 120.2(7)
	O(8)−C(49)−N(8) 120.2(3)	C(1)−C4)−C(2) 120.4(7)				

[a] Φ is the twist angle between the Mo_2 axes. [b] For **2** and **6**, X(1) = O(1), X(2) = N(13), X(3) = O(2), X(4) = N(14); for **1**, **3** − **5**, X(1) = N(7), X(2) = O(7).

aromatic C−H), 6.50 (s, 1H, pyrimidinate C−H), 6.45 (d, 4H, aromatic, C−H), 6.17−6.32 (m, 16H, aromatic C−H), 6.09 (d, 8H, aromatic C−H), 5.96 (d, 4H, aromatic C−H), 3.71 (s, 12H, −OC*H*$_3$), 3.64 (s, 6H, −OC*H*$_3$), 3.59 (s, 18H, −OC*H*$_3$). Absorption spectrum (CH_2Cl_2) λ_{max} (ϵ_M): 269 (106 000), 295 (103 000), 337 (sh, 62 800), 405 (sh, 10 600), 469 (4270). Anal. Calcd for $[Mo_2(DAniF)_3]_2$(μ-4,6-dioxypyrimidinate)·0.5CH_2Cl_2, $C_{99.5}H_{93}Cl_1Mo_4N_{14}O_{14}$: C, 54.88; H, 4.53; N, 9.48. Found: C, 54.80; H, 4.58; N, 9.54%.

$[Mo_2(DAniF)_3]_2$(μ-2,3-dioxy-1,4-pyrazinate) (3). Yield: yellow-orange needles, 42%. ^{1}H NMR (ppm in CD_2Cl_2): 8.53 (s, 2H, −NC*H*N−), 8.40 (s, 4H, −NC*H*N−), 7.87 (dd, 1H, aromatic C−H), 6.18−6.67 (m, 48H, aromatic C−H), 5.99(dd, 1H, aromatic, C−H), 3.73 (s, 6H, −OC*H*$_3$), 3.68 (s, 12H, −OC*H*$_3$), 3.67 (s, 12H, −OC*H*$_3$), 3.64 (s, 6H, −OC*H*$_3$). Absorption spectrum (CH_2Cl_2) λ_{max} (ϵ_M): 267 (104 000), 294 (106 000), 420 (16 100), 477 (14 000). Anal. Calcd for $C_{94}H_{92}Mo_2N_{14}O_{14}$: C, 55.74; H, 4.58; N, 9.68. Found: C, 54.53; H, 4.59; N, 9.46%.

$[Mo_2(DAniF)_3]_2$(μ-2,3-dioxyquinoxalinate) (4). Yield: orange blocks, 43%. ^{1}H NMR (ppm in CD_2Cl_2): 8.64 (s, 2H, −NC*H*N−), 8.35 (s, 4H, −NC*H*N−), 6.54−6.70 (m, 20H, aromatic C−H), 6.41−6.48 (m, 20H, aromatic C−H), 6.33(d, 4H, aromatic C−H), 6.24 (d, 4H, aromatic C−H), 6.19 (d, 2H, aromatic C−H), 4.53 (m, 2H, aromatic C−H), 3.74 (s, 6H, −OC*H*$_3$), 3.67 (s, 12H, −OC*H*$_3$), 3.65 (s, 62H, −OC*H*$_3$), 3.64 (s, 6H, −OC*H*$_3$). Absorption spectrum (CH_2Cl_2) λ_{max} (ϵ_M): 267 (sh, 106 000), 278 (107 000), 306 (100 000), 447 (sh, 12 100), 479 (15 200), 511 (sh, 11800). Anal. Calcd for $C_{98}H_{94}Mo_4N_{14}O_{14}$: C, 56.71; H, 4.56; N, 9.45. Found: C, 56.87; H, 4.59; N, 9.39%.

$[Mo_2(DAniF)_3]_2$(μ-2,3-dicyano-5,6-dioxypyrazinate) (5). Yield: violet blocks, 35%. ^{1}H NMR (ppm in CD_2Cl_2): 8.65 (s, 2H, −NC*H*N−), 8.42 (s, 4H, −NC*H*N−), 6.42−6.68 (m, 36H, aromatic C−H), 6.44 (d, 4H, aromatic C−H), 6.30 (d, 4H, aromatic C−H), 6.20 (d, 4H, aromatic C−H), 3.72 (s, 6H, −OC*H*$_3$), 3.70 (s, 12H, −OC*H*$_3$), 3.68 (s, 12H, −OC*H*$_3$), 3.64 (s, 6H, −OC*H*$_3$). Absorption spectrum (CH_2Cl_2) λ_{max} (ϵ_M): 258 (89 600), 280 (89 500), 300 (88 100), 344 (sh, 48 000), 484 (sh, 11 600), 513 (14 200), 550 (12 300). Anal. Calcd for $C_{96}H_{90}Mo_4N_{64}O_{14}$: C, 55.55; H, 4.37; N, 10.79. Found: C, 55.50; H, 4.45; N, 10.58%.

$[Mo_2(DAniF)_3]_2$(μ-cyanurate) (6). Yield: yellow plates, 53%. ^{1}H NMR (ppm in TDF): 8.66 (s, 4H, −NC*H*N−), 8.20 (s, 2H, −NC*H*N−), 6.76 (d, 8H, aromatic C−H), 6.58−6.63 (m, 16H, aromatic C−H), 6.48 (d, 8H, aromatic C−H), 6.40 (d, 4H, aromatic C−H), 6.24 (d, 4H, aromatic C−H), 6.10 (d, 4H, aromatic C−H), 5.84 (d, 4H, aromatic C−H), 3.66 (s, 12H, −OC*H*$_3$), 3.59 (s, 12H, −OC*H*$_3$), 3.58 (s, 6H, −OC*H*$_3$), 3.51 (s, 6H, −OC*H*$_3$). The resonance for the N−H hydrogen of the cyanurate linker was obscured in this spectrum. MS ESI$^+$: 1021 (MH_2^{2+}/2), 1086 (MH^+ − $Mo_2(DAniF)_3$).

Results and Discussion

Syntheses. The method of synthesis involves reduction of the mixed valent $Mo_2(DAniF)_3Cl_2$ compound with Zn metal in acetonitrile (eq 1) followed by an *in situ* reaction with the corresponding dianion of the linker, L, as its Et_4N^+ salt, as shown in eq 2:

$$2Mo_2(DAniF)_3Cl_2 + Zn + 4MeCN \rightarrow [Mo_2(DAniF)_3(MeCN)_2]_2ZnCl_4 \quad (1)$$

$$2[Mo_2(DAniF)_3(MeCN)_2]^+ + L^{2-} \rightarrow (DAniF)_3Mo_2-L-Mo_2(DAniF)_3 \quad (2)$$

The neutral linked complexes generally precipitate directly from acetonitrile solution as microcrystalline solids that are conveniently isolated by filtration. Although air-sensitive in solution, these compounds are moderately stable to air as solids but are best stored for prolonged periods of time under N_2.

In the particular case of uracilate, it was found that the 1:1 adduct, **1**, was the only species isolated regardless of whether the mono- or dianion was used and despite variation in the stoichiometry of the uracilate dianion that was employed. This result appears to be due to the prohibitive steric congestion that would arise from the juxtaposition of the two $Mo_2(DAniF)_3^+$ units about the uracilate core, a point which is illustrated schematically in Figure 1a. In this context, the futility of attempting to employ 3,6-dihydroxypyradizine (*E* in Scheme 3 (IIIa)) as a linking ligand is patently obvious. As shown in Figure 1a, 3,6-dihydroxypyradizine would produce even more steric crowding between two $Mo_2(DAniF)_3^+$ units than does

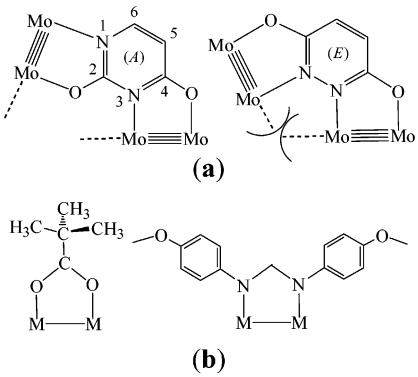

Figure 1. (a) Relative disposition of the Mo_2 units with diamidate ligands *A* and *E*. (b) Relative steric requirements of the pivalate and DAniF ligands.

uracilate, so its use as a linker was not attempted here. We note that Chisholm *et al*. have succeeded in bridging two Mo_2^{4+} units with the dianion of 3,6-dihydroxypyradizine.[29] In this system, however, the sterically less demanding pivalate ion was employed as supporting ligand on the Mo_2 units; the comparative steric requirements of the two ligands are made clear in Figure 1b.

Structures. The core structures of molecules **1**−**6** are presented in Figure 2 with 50% probability ellipsoids and all *p*-anisyl substituents and hydrogen atom omitted for clarity except for the N−H hydrogen atoms in **1** and **6**. Cell parameters and refinement statistics for all the structures are presented in Table 1, while selected bond distances and angles are collected in Tables 2 and 3, respectively. The separation between the centroids of the Mo_2^{4+} units, *d*, for **2**−**6** falls within the relatively narrow range 7.08−7.32 Å, thus permitting an assessment of the effects of the linker in mediating electronic communication at approximately constant *d* (*vide infra*).

Compound **1** was the species isolated and crystallized in attempts to prepare a linked molecule, but it is merely one isomer of the two conceivable ones which might arise in the formation of a 1:1 adduct between $Mo_2(DAniF)_3^+$ and uracilate. Furthermore, as revealed by ^{1}H NMR, **1** is stable in CH_2Cl_2 solution and does not exist in equilibrium with the isomer in which N1 of uracil is coordinated to molybdenum (see Figure 1a for numbering scheme). The N3 proton which has been removed is the less acidic of the two ($pK_a = 9.43$,[30] although the difference in relative acidity between the two sites is only slight), suggesting that coordination at N3 is preferred because it is the more basic site. The origin of the proton on N1 of the uracilate ligand (N8 in Figure 2) may be due to either incomplete deprotonation by 2 equiv of Et_4NOH ($pK_a = 13.5$ for the second deprotonation) or perhaps incomplete drying of the $(Et_4N)_2$-(uracilate) salt once it is formed. The position of H(8A) in **1** (Figure 2) was visible in the final difference maps and was permitted to refine.

The transition metal coordination chemistry of uracilate has been rather unevenly explored but is perhaps furthest developed for Pt^{II}, where, among the more notable achievements that have been reported, uracilate has served as a linker in the formation of cationic squares with $(en)Pt^{2+}$ corner endpieces.[31] Compound **1** appears to be the only structurally characterized molybdenum complex with a uracilate ligand[32] as well as the first in which uracilate serves as a bridging ligand between two multiply bonded metal atoms. The closely related 1-methyl uracilate ligand, however, has been reported in a similar N−C−O binding mode in several diplatinum(III,III) compounds in which at least a formal Pt−Pt single bond exists.[33]

Compound **2** is the first structurally characterized compound in which the anion of 4,6-hydroxypyrimidine is a ligand to any sort of transition metal. The only prior study of the coordination chemistry of this particular ligand deals with measurements of the stability constants of the complexes formed with Co^{II}, Mn^{II}, Ni^{II}, and Zn^{II} without isolation and physical characterization of the species formed.[34] The significant twist angle of 35.9° (Table 3) between the two Mo_2 axes is readily apparent in the thermal ellipsoid drawing in Figure 2. The eight non-hydrogen atoms of the dioxypyrimidinate linker have a mean deviation of 0.0674 Å from the mean plane which they define, with the greatest deviation being 0.164 Å for N(14). The appreciable distortion observed in the crystal structure of **2** may be plausibly attributed to crystal packing effects since it is the only compound in the set which crystallizes without solvent in the lattice and since it has virtually the same size and shape as **6**, which has an essentially planar core.

Compounds **3**−**5** are related inasmuch as the linking ligands all contain the 2,3-dioxypyrazine core. All three molecules have essentially planar core structures with little (5.1° for **5**) or no (for **3** and **4**) twist between the Mo_2 axes. Molecules **3** and **4** crystallize upon inversion centers in the space group $P\bar{1}$ with the result that the linking ligand is seen as a 1:1 overlay of two orientations in which the oxygen and nitrogen atoms are interchanged. For convenience, this disorder may be envisioned by imagining **3** and **4** to be fixed and then rotating the 2,3-dioxypyrazinate or 2,3-dioxyquinoxalinate ligand 180° around the C47−C47A or C1−C1A axis, respectively, to generate its other positional variant. This imposed disorder introduces large uncertainties into the bond parameters of these linking ligands (Tables 2 and 3). In the case of **4**, this disorder necessitated restraining the N(7)−C(1) and O(7)−C(1) bond distances to chemically reasonable values. In compound **5**, there is a 2-fold axis bisecting the C(46)−C(46A) bond and extending parallel to the Mo(1)−Mo(2) axis, thereby generating the right half of the molecule from the left. This symmetry element, however, does not generate the type of disorder observed in **3** and **4**.

Compound **3** is the only structurally characterized transition metal complex with 2,3-dioxypyrazine in any coordination mode and, furthermore, appears to be the first structurally characterized molecule, organic or inorganic, which contains the 2,3-dioxypyrazine fragment. The closest related structures which occur in the Cambridge Structural Database are those with the 2,3-piperazinedione core,[35] where the C−C bond of the aryl ring (C46−C48 in **3**) has been reduced to a single bond. A molecule closely related to **4**, again with the pivalate anion as supporting

(29) Cayton, R. H.; Chisholm, M. H.; Putilina, E. F.; Folting, K. *Polyhedron* **1993**, *12*, 2627.
(30) Jonáš, J.; Gut, J. *Collect. Czech. Chem. Commun.* **1962**, *27*, 716.
(31) (a) Rauter, H.; Hillgeris, E. C.; Lippert, B. *Chem. Commun.* **1992**, 1385. (b) Rauter, H.; Hillgeris, E. C.; Erxleben, A.; Lippert, B. *J. Am. Chem. Soc.* **1994**, *116*, 616. (c) Navarro, J. A. R.; Freisinger, E.; Lippert, B. *Eur. J. Inorg. Chem.* **2000**, 147.
(32) The only other molybdenum complex with uracilate as a ligand which can be found in the literature was not structurally characterized: Dias, A. R.; Duarte, M. T.; Galvão, A. M.; Garcia, M. H.; Marques, M. M.; Salema, M. S. *Polyhedron* **1995**, *14*, 675.
(33) (a) Lippert, B.; Schöllhorn, H.; Thewalt, U. *Inorg. Chem.* **1986**, *25*, 407. (b) Schöllhorn, H.; Eisenmann, P.; Thewalt, U.; Lippert, B. *Inorg. Chem.* **1986**, *25*, 3384.
(34) Sengupta, S.; Bannerjee, N. R. *J. Ind. Chem. Soc.* **1990**, *67*, 313.

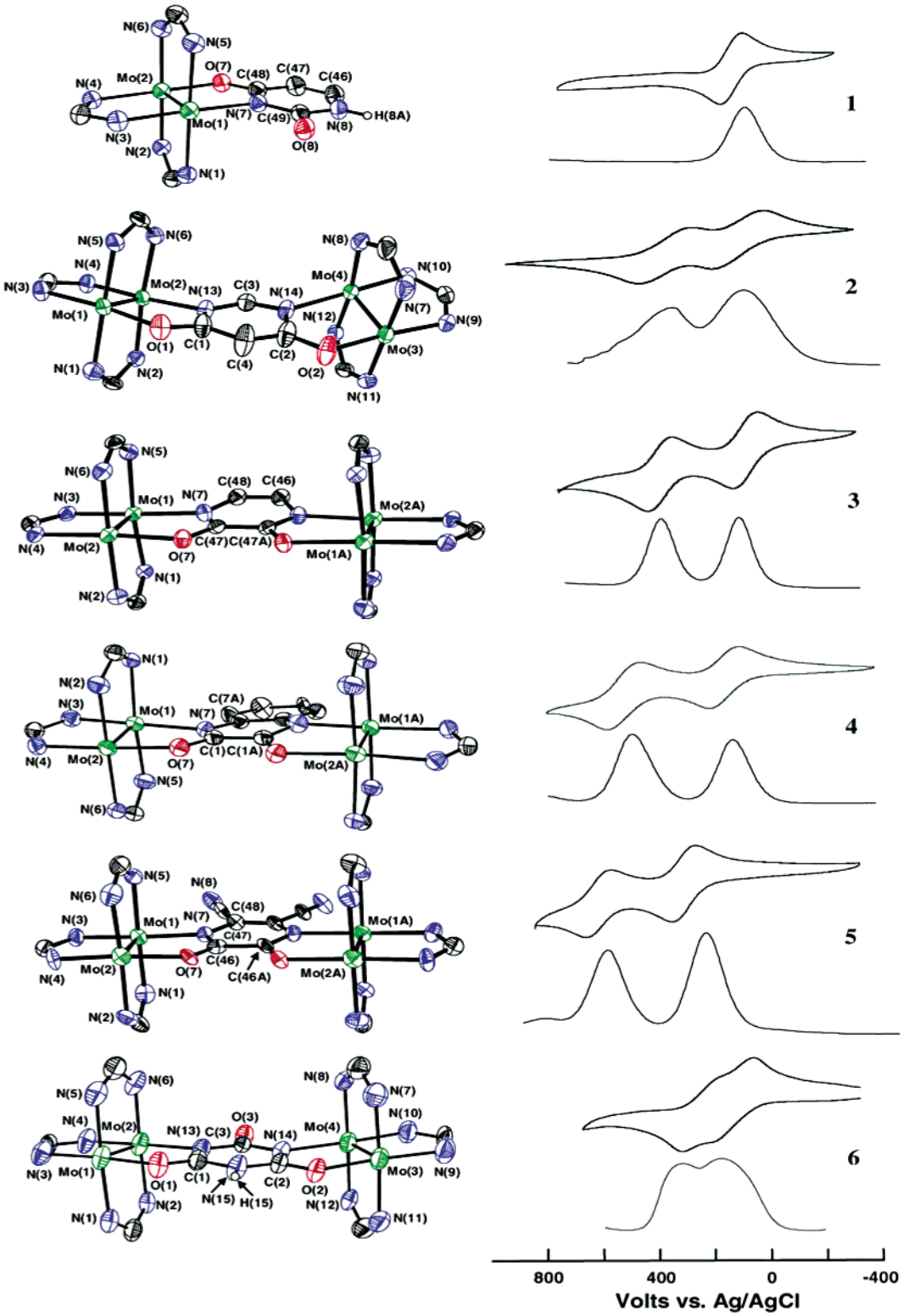

Figure 2. The core structures of the six polyamido molybdenum compounds. Displacement ellipsoids are drawn at the 50% probability level. The *p*-anisyl groups attached to the N atoms and all hydrogen atoms are omitted for clarity, except for H(8A) on **1** and H(15) in **6**. To the right of each structure, the number of each compound, the cyclic voltammogram (above) and the differential pulse voltammogram (below) are shown. These electrochemical measurements were recorded in CH_2Cl_2 solutions.

ligand, was previously reported by Chisholm *et al.*[2,29] although it was not structurally characterized by X-ray diffraction. Compound **4** is the first crystallographically characterized example of a transition metal complex in which 2,3-dioxyquinoxalinate coordinates in the N−C−O amidate mode rather than as an ene-1,2-diolate ligand. The only other crystallographically characterized transition metal complexes with this ligand, $[Fe^{III}$-(2,3-dioxyquinoxalinate)$_3]^{3-}$ [36] and Cp*Ru(NO)(2,3-dioxyquinoxalinate),[37] display the latter binding mode. Molecule **5**, like **4**, is the sole instance of a structurally characterized transition

metal compound in which its ligand coordinates in the amidate motif rather than as an ene-1,2-diolate ligand. The transition metal chemistry of 2,3-dioxy-5,6-dicyanopyrazine is quite scant and limited to a few reports describing its utility in the formation of extended two-dimensional structures with Cu^{II}.[38]

The coordination chemistry of cyanuric acid (*H* in Scheme 3a) is confined to simple monodentate O- or N-bound complexes with middle and late first row transition metal ions, principally Co^{III},[39] Mn^{II},[39] Cu^{II},[40] and Ni^{II}.[41] Compound **6** is thus the only crystallographically characterized complex of this ligand with molybdenum, the sole example in which cyanurate is coordinated to any sort of M_2 unit and, furthermore, the only case in which the N−C−O amidate coordination mode is observed for this ligand. The core structure of **6** is essentially planar, in contrast to that of **2**, with only a slight twist angle of 3.2° between the Mo_2 units. The short C(3)−O(3) bond distance of 1.211(9) Å in the cyanurate ligand is indicative of a double bond. The diffraction data for this compound was of a quality sufficient to reveal the presence of the hydrogen atom bound to N(15), and its position was refined. It is clear that the same steric considerations that preclude formation of a linked species with the uracilate dianion (Figure 1a) also render impossible the formation of the trigonally symmetric molecule $[Mo_2(DAniF)_3]_3(\mu^3$-cyanurate).

The structures of three of the molecular precursors of the six linking ligands, namely uracil,[42] 1,4-dihydro-2,3-quinoxalinedione,[43] and cyanuric acid,[44] have been previously described and provide useful comparisons for assessing the tautomeric form of the ligand anions as coordinated to the Mo_2 unit. These three neutral ligands all exist in the keto amine tautomeric form in the crystalline state, a formulation born out by the short carbon−oxygen bond distances and by the visibility of the hydrogen atoms themselves on the nitrogen atoms in the electron density maps. In the corresponding Mo_2 compounds, the carbon oxygen bond lengths are substantially lengthened, while the carbon nitrogen bond lengths are relatively unaffected. In compounds **3** and **4**, it should be noted that the previously described crystallographic disorder renders these bond distances considerably less reliable then those in the other compounds. Taken as a whole, however, the structural results support a description of the ligand anions as enolate type anions rather than as keto aminate anions.

Electrochemistry. The electrochemical results are presented graphically in Figure 2 and summarized numerically in Table 4. The compounds with pyrazine-type linkers, **3**−**5**, all have

Table 4. Electrochemical Data[a] for Compounds **1** − **6**

	peak positions[b] (mV) $E_{1/2}$ (1+/0)	$\Delta E_{1/2}$(mV) $E_{1/2}$ (2+/1+)	K_c[c]	
1	172			
2	99	286	187	1.5×10^3
3	131	389	258	2.3×10^4
4	156	464	308	1.6×10^5
5	339	602	263	2.8×10^4
6	272	424	152	3.7×10^2

[a] All potentials are referenced to Ag/AgCl. Data for **1**−**5** are from CH_2Cl_2 solutions, while data for **6** are from a THF solution; $E_{1/2}$ for Fc^+/Fc is +440 mV in CH_2Cl_2 and +574 mV in THF. [b] $E_{1/2} = (E_{pa} + E_{pc})/2$ from the CV. [c] K_c is calculated from the formula $K_c = e^{\Delta E_{1/2}/25.69}$.

Table 5. Electrochemical Data for Selected Linked Pairs of Mo_2^{4+} Units

	peak positions (mV)				
	$E_{1/2}$ (1+/0)	$E_{1/2}$ (2+/1+)	$\Delta E_{1/2}$ (mV)	K_c[c]	reference
$[Mo_2(DAniF)_3]_2(\mu\text{-}O_2CCO_2)$	+294	+506	212	3.8×10^3	5a,c
$[Mo_2(DAniF)_3]_2(\mu\text{-}SO_4)$	+93	+321	228	7.2×10^3	10
$[Mo_2(DAniF)_3]_2(\mu\text{-}MoO_4)$	+81	+392	311	1.8×10^5	10
$[Mo_2(DAniF)_3]_2(\mu\text{-}WO_4)$	+102	+387	285	6.6×10^4	10
$[Mo_2(DAniF)_3]_2(\mu\text{-}Cl)_4$	+271	+798	527	8.1×10^8	*a*
$[Mo_2(DAniF)_3]_2(\mu\text{-}Zn(OMe)_4)$	−208	30	238	1.1×10^4	*b*
$[Mo_2(DAniF)_3]_2(\mu\text{-}Co(OMe)_4)$	−205	60	265	3.0×10^4	*b*
$[Mo_2(DAniF)_3]_2(\mu\text{-fluoflavinate})$	+140	+1020	880	7.5×10^{14}	*a*

[a] Unpublished data. [b] Cotton, F. A.; Liu, C. Y.; Murillo, C. A. *Inorg. Chem.* **2003**, *42*, in press.

$\Delta E_{1/2}$ values sufficiently high as to permit their determination as $E^{(2)}{}_{1/2} - E^{(1)}{}_{1/2}$ in a straightforward manner directly from the cyclic voltammograms. The pyrazinate linkers in **3**−**5** are all more effective than oxalate (See Table 5) in delocalizing charge in the mixed valent species and thereby mediating electronic communication between the two Mo_2 units. These $\Delta E_{1/2}$ values are ∼45, ∼95, and ∼50 mV greater, respectively, than that of the oxalate linked molecule despite having slightly greater values of *d* ($d = 6.953$ Å for $[Mo_2(DAniF)_3]_2(\mu\text{-}O_2CCO_2)$ (see Table 5)). Comparing **4** and **5**, one observes that benzannulation of the pyrazine ring has a significantly greater effect upon $\Delta E_{1/2}$ than substitution with cyano groups. Compound **4** therefore represents the best candidate in this series for the successful isolation of a one-electron oxidized species and is the object of current research in this laboratory. We note that Chisholm's analogue to **4**,[29] which has $Mo_2(O_2CCMe_3)$ units in lieu of $Mo_2(DAniF)_3$ units, has a $\Delta E_{1/2}$ of 366 mV rather than 308 mV. This difference corresponds to an order of magnitude increase in K_c (1.5×10^6) over our compound **4** (1.6×10^5). For molecule **5**, the $E^{(1)}{}_{1/2}$ and $E^{(2)}{}_{1/2}$ values are shifted approximately 200 mV to more strongly oxidizing potentials relative to **3** due to the highly electron withdrawing nature of the cyano groups. The potentials for **4** are also shifted toward higher values relative to **3**, but as one might anticipate, the effect is much less pronounced since **4** has only the effect of increased delocalization but not the inductive influence of the highly electron withdrawing cyano substituents.

Compound **2** is a significantly poorer mediator of the effect of oxidation of one Mo_2 unit upon the other, with a $\Delta E_{1/2}$ of 187 mV. This point is further underscored by considering that, since **2** is a relatively rigid molecule and its structure in the crystalline state and in solution ought to be essentially the same, a more meaningful value for **d** in the context of understanding the electrochemistry is the distance between Mo(2) and Mo(4)

(35) For instance, see: (a) Lenstra, A. T. H.; Bracke, B.; van Dijk, B.; Maes, S.; Vanhulle, C.; Desseyn, H. O. *Acta Crystallogr.* **1998**, *B54*, 851. (b) Bellouard, F.; Chuburu, F.; Kervarec, N.; Toupet, L.; Triki, S.; Le Mest, Y.; Handel, H. *J. Chem. Soc., Perkin Trans. 1* **1999**, 3499.
(36) Muñoz, M. C.; Ruiz, R.; Traianidis, M.; Aukauloo, A.; Cano, J.; Journaux, Y.; Fernández, I.; Pedro, J. R. *Angew. Chem., Int. Ed. Engl.* **1998**, *37*, 1834.
(37) Yang, K.; Bott, S. G.; Richmond, M. G. *J. Chem. Cryst.* **1995**, *25*, 283.
(38) Adachi, K.; Sugiyama, Y.; Kumagai, H.; Inoue, K.; Kitagawa, S.; Kawata, S. *Polyhedron* **2001**, *20*, 1411.
(39) Falvello, L. R.; Pascual, I.; Tomás, M. *Inorg. Chim. Acta* **1995**, *229*, 135.
(40) (a) Falvello, L. R.; Pascual, I.; Tomás, M.; Urriolabeitia, E. P. *J. Am. Chem. Soc.* **1997**, *119*, 11894. (b) Hart, R. D.; Skelton, B. W.; White, A. H. *Aust. J. Chem.* **1992**, *45*, 1927. (c) Server-Carrio, J.; Folgado, J.-V. *Polyhedron* **1998**, *17*, 1495.
(41) (a) Palade, T.; Nutiu, M. *Rev. Chim.* **1986**, *37*, 80. (b) Falvello, L. R.; Pascual, I.; Tomás, M. *Inorg. Chim. Acta* **1995**, *229*, 135, (c) Falvello, L. R.; Hitchman, M. A.; Palacio, F.; Pascual, I.; Schultz, A. J.; Stratemeier, H.; Tomás, M.; Urriolabeitia, E. P.; Young, D. M. *J. Am. Chem. Soc.* **1999**, *121*, 2808.
(42) Stewart, R. F.; Jensen, L. H. *Acta Crystallogr.* **1967**, *23*, 1102.
(43) Svensson, C. *Acta Chem. Scand.* **1976**, *B30*, 581.
(44) Coppens, P.; Vos, A. *Acta Crystallogr.* **1971**, *B27*, 146.

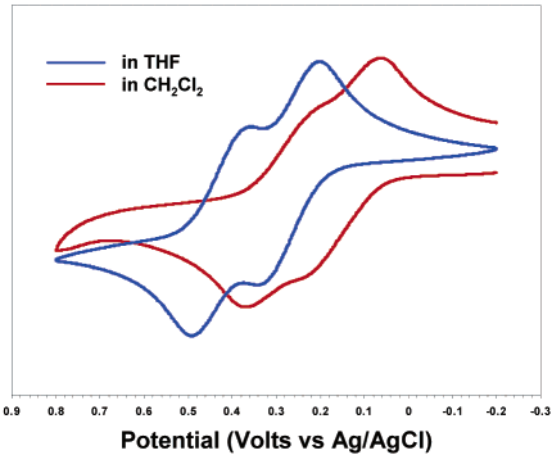

Figure 3. Comparison of the cyclic voltammetry of **6** in THF (blue trace) vs CH_2Cl_2 (red trace).

(6.357 Å in Figure 2) since that value represents the closest approach of the Mo_2 units. Despite having the ends of the Mo_2 units substantially closer to one another than **3**−**5** and arguably contributing more to $\Delta E_{1/2}$ through electrostatic or through-space effects, **2** still has a substantially lower $\Delta E_{1/2}$. Within the present set of compounds, no comparisons can be made which would separate the relative contributions of electrostatic and orbital coupling effects.

The electrochemical traces for compound **6** are atypically broad, most notably in the differential pulse voltammogram of Figure 2, and suggest that the interpretation of its electrochemistry is not as straightforward as it is with the other compounds. The ^{1}H NMR spectroscopy of **6** indicates a complex solution behavior for this molecule which is not observed for **1**−**5**. At least three distinct species appear to be present in significant amounts in dichloromethane solution even when highly crystalline samples of **6** are used. The origin and identities of these species are unclear, but possible explanations include the existence of an equilibrium between N−H and O−H tautomers of the μ-cyanurate linker, partial dissociation of **6** into unlinked species, and/or the formation of N-chloro cyanurate species in the presence of chloroalkanes.[45] The ^{1}H NMR spectrum in deuterated THF indicates that formation of other species is largely suppressed although not completely eliminated in this solvent. This point is corroborated by the observation of significantly better resolved electrochemical traces for **6** when these measurements are repeated in THF rather than CH_2Cl_2 (Figure 3). The values for **6** in Table 4 are those obtained from a THF solution.

Electronic Spectra and Structures. In our preceding study of the spectra and electronic structures of compounds of type Ib with polyunsaturated dicarboxylate linkers,[46] time-dependent DFT calculations revealed the lowest energy absorptions to be HOMO → LUMO excitations which were essentially Mo_2 δ → dicarboxylate π^* metal-to-ligand charge transfers. These features in the electronic spectra were noteworthy because they were significantly lower in energy and higher in intensity than the $\delta \rightarrow \delta^*$ transition typically observed as the lowest energy

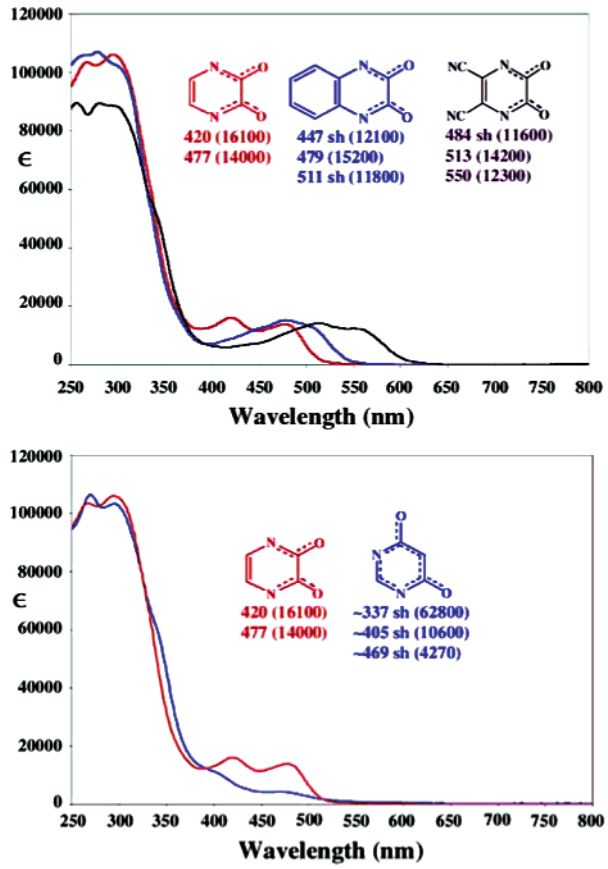

Figure 4. UV−vis spectra in CH_2Cl_2 of selected compounds as identified by their cyclic polyamidate linker. (Upper panel) Spectra of the three compounds with pyrazine-type linkers. (Lower panel) Comparison of the two structural isomers with 2,3-dioxypyrazinate (red) and 4,6-dioxypyrimidinate (blue) as linkers.

feature in individual Mo_2 quadruply bonded compounds with a ground state electronic configuration of $\sigma^2\pi^4\delta^2$. This $\delta \rightarrow \delta^*$ transition, also known as $^1A_{1g} \rightarrow {}^1A_{2u}$, is due to the excitation of one electron to the $\sigma\pi\delta\delta^*$ state and is intrinsically weak due to the small overlap integral between δ orbitals, even though such transitions are symmetry allowed.[47] For example, when the ligands are carboxylate, sulfate, or water, the intensities of the $\delta \rightarrow \delta^*$ transition have ϵ_{max} values of a few hundreds up to ~1000. The intensities can increase but usually by not much more than a factor of 2 when mixing with MLCT transitions occurs.

The absorption spectra of the cyclic polyamidate linked molecules **2**−**5** were initially expected to be very similar to the polyunsaturated dicarboxylate linked compounds of type Ib but instead were observed to display significant differences (Figure 4). The electronic spectra of **3**, **4**, and **5** (Figure 4, upper panel) reveal at least two low energy features of comparable intensity. These features are well resolved in **3** and less so in **4** and **5**. In **4**, it appears that three distinct absorptions exist, two of which merely appear as shoulders. The transitions responsible for these colors must involve orbitals of the pyrazinate linker since that is the only variable being changed in this set of compounds. The pronounced shift to lower energy in moving from **3** to **5** accords with the intuitive expectation that the energy of the π

(45) Elemental analyses upon samples of **6** which have been dissolved in CH_2Cl_2 and evaporated to dryness indicate the presence of substantial amounts of residual chlorine.
(46) Cotton, F. A.; Donahue, J. P.; Murillo, C. A.; Pérez, L. M. *J. Am. Chem. Soc.* **2003**, *125*, 5486.
(47) Cotton. F. A.; Walton, R. A. *Multiple Bonds between Metal Atoms*; Clarendon: Oxford, 1993.

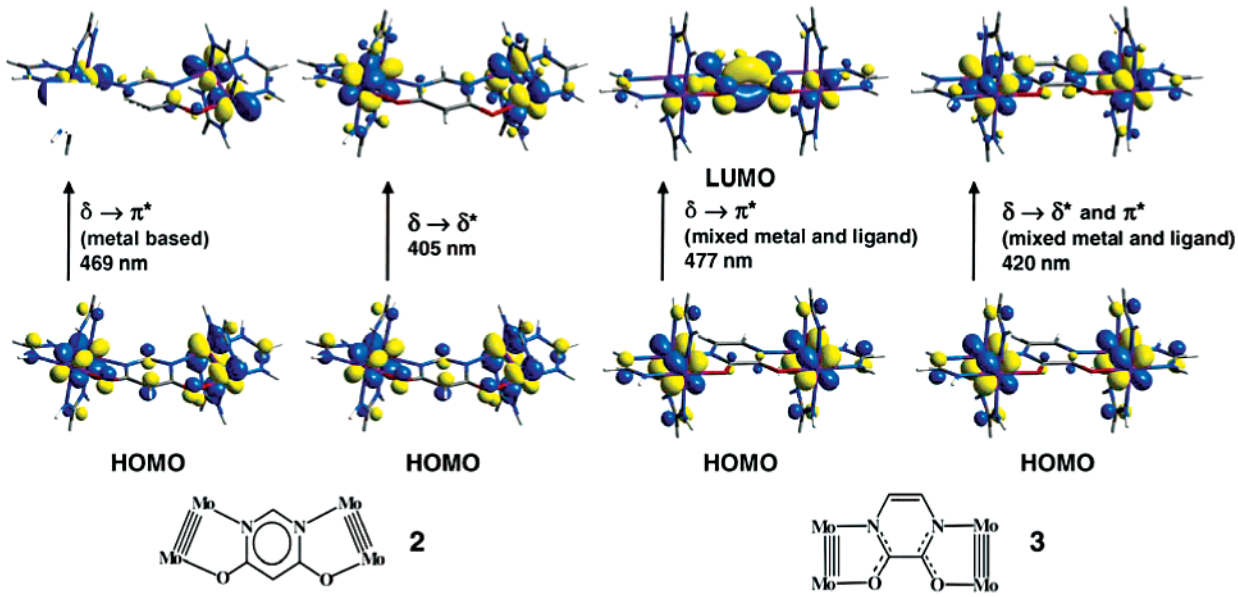

Figure 5. Illustration of the 0.04 contour surface diagram of the time-dependent DFT calculated molecular orbital responsible for the two lowest energy transitions in molecules **2** and **3**. In the case of **2**, the MOs involved are primarily metal based. For **3**, substantial mixing occurs between the molybdenum atoms and the diamidate linking ligand. The lowest energy transition in **3** is a HOMO → LUMO transition.

system of the pyrazine core would be lowered by benzannulation to form the quinoxaline system and by substitution with highly electron withdrawing cyano groups in **5**. A second interesting comparison to note is that between molecules **2** and **3** (Figure 4, lower panel). The significant differences in their absorption maxima and band intensities suggest the involvement of molecular orbitals of substantially different composition.

Time-dependent DFT calculations upon molecules **2** and **3** were undertaken to obtain at least a qualitative insight into the nature of the absorption bands shown in Figure 4. The results indicate that not only are **2** and **3** quite different from the polyunsaturated dicarboxylate linked molecules such as $[Mo_2(DAniF)_3]_2(\mu\text{-}trans\text{-}O_2CCH{=}CHCO_2)$ but also that they are qualitatively quite different from one another despite being structural isomers. The absorption band observed at 477 nm for **3**, which is the HOMO → LUMO excitation, is a $\delta \rightarrow \pi^*$ charge transfer with a substantial metal contribution to the composition of the π^* orbital (Figure 5, right side). The higher energy transition in **3** is an excitation from the HOMO (essentially the Mo_2 δorbital) to an MO which is largely δ^* in character but which also has an appreciable amount of ligand π^* character mixed into it from the diamidate linker.

In contrast, the two lowest energy bands in **2** are both metal based and have relatively little involvement from the dioxypyrimidinate linker. This fact explains the significant decrease in intensity of these two shoulders at 469 and 405 nm relative to the absorptions in **3** since metal-to-ligand charge transfer bands generally have much higher extinction coefficients due to more efficient electron density shifts between the orbitals involved. The lowest energy band in **2** involves a $\delta \rightarrow \pi^*$ transition, but the π^* orbital is essentially metal based and can be clearly seen as the out of phase interaction of the d_{xz} orbitals of the two Mo_2 units in **2** (Figure 5, left side). DFT results indicate that the shoulder at 405 nm in **2** may be assigned as the Mo_2 $\delta \rightarrow \delta^*$ transition. This dramatic difference between the electronic absorption spectra of **2** and **3**, which are structural isomers, is a result which in hindsight finds an intuitive grasp in considering the difference between the aromatic systems of the 2,3-dioxypyrazine and 4,6-dioxypyrimidine rings. For the latter ring system, the *meta* disposition of the ring nitrogen atoms and the oxy substituents limits the resonance forms that can be drawn for this ligand as compared to the 2,3-dioxypyrazine ligand. Apparently this affects the energetics or the symmetry or both of the π system, possibly because of a discontinuity introduced by the presence of a node(s), such that the δ orbitals of the Mo_2 units can no longer effectively interact with it.

Summary and Conclusions

The present work extends the family of linked pairs of $Mo_2(DAniF)_3$ units, which until now has been comprised of molecules joined by dicarboxylates ($^-O_2CXCO_2^-$), tetrahedral oxo anions (EO_4^{2-}, E = S, Mo, and W), and *N,N′*-diarylterephthaloyldiamidate linkers, to include a distinctly new set of compounds with cyclic diamidate linkers. With uracilate as potential linker, only the 1:1 adduct $Mo_2(DAniF)_3$(uracilate), **1**, is formed for steric reasons. Similarly, cyanurate is capable of coordinating only two $Mo_2(DAniF)_3$ units rather than three in a trigonally symmetric fashion. The uncoordinated nitrogen of the cyanurate ligand is found to be the site of the remaining proton.

In the set of compounds **1**−**6**, there is a surprising number of firsts in the transition metal chemistry of these diamidate ligands. In addition to being a rare instance of a structurally characterized uracilate complex of molybdenum, **1** is also a unique example in which uracilate spans two multiply bonded metal atoms. Compounds **2** and **3**, with 4,6-dioxypyrimidinate and 2,3-dioxypyrazinate, are the only well-characterized transition metal complexes of any kind with these ligands. No molecule, organic or inorganic, has been previously characterized with the 2,3-dioxypyrazinate core. Compound **5** represents the first structurally characterized complex of 2,3-dioxy-5,6-dicyanopyrazinate binding as an amidate type ligand. An analogue of **4** has been previously described by Chisholm, but its crystal structure was not reported. To the best of our

knowledge, compound **6** represents a new coordination mode for cyanurate, all prior examples being limited to simple monodentate N-bound or O-bound complexes with this ligand.

The cyclic voltammograms of **3**−**5** ($\Delta E_{1/2}$ = 258, 308, 263 mV, respectively) reveal that they are substantially better mediators of electronic communication than even the oxalate-linked molecule. By the Robin−Day classification scheme,[48] the one electron oxidized form of **4** would represent a type III fully delocalized system. It is undoubtedly the case that the π system of the pyrazinate ring is intimately involved in facilitating this charge delocalization. In contrast, the electrochemistry of **2**, although it is a structural isomer of **3**, is significantly less effective in mediating communication, an effect which may be attributable to the different symmetry of the 4,6-dioxypyrimidinate ring. Compound **6** has been found to have a rather complex and unexpected solution behavior that displays a strong solvent dependence. In THF, however, a single species preponderates.

The electronic absorption spectra of **3**−**5** are in many respects consistent with the electrochemistry in supporting the idea that these compounds are in fact quite different than their dicarboxylate linked congeners. In particular, they have two or three, rather than one, features in the 420−550 nm region. Compound **2** has two unresolved shoulders of appreciably lower intensity than the absorption bands in **3**−**5**. Time-dependent DFT calculations on **3** identify its lowest energy band as a $\delta \rightarrow \pi^*$ transition, where the π^* orbital has appreciable metal as well as diamidate ligand character. This excitation is the HOMO → LUMO transition. The higher energy absorption in **3** involves a transition from the δ orbital to an MO which has mixed δ^* and π^* character to it. Unlike **3**, the two lowest energy features in **2** both appear to be metal based, the lower energy one being a $\delta \rightarrow \pi^*$ type transition while the other is essentially a $\delta \rightarrow \delta^*$ excitation. The electronic spectra and DFT calculations reinforce the observation from the electrochemistry results that **2** and **3** are in fact very different electronically and that the latter, probably for symmetry reasons, is somewhat better than the former in mediating electronic communication. These cyclic polyamidate linker pairs bear little resemblance to their *N*,*N*′-diarylterephthaloyldiamidate linked analogues and must be regarded as a distinctly different type of compound.

Acknowledgment. This research was supported by the National Science Foundation and the Robert A. Welch Foundation. J.P.D. gratefully acknowledges the support of an NIH postdoctoral fellowship.

Supporting Information Available: Thermal ellipsoid drawings at the 50% probability level with complete atomic labeling in PDF in addition to X-ray crystallographic data for compounds **1**−**6** in CIF format. This material is available free of charge via the Internet at http://pubs.acs.org.

JA0358044

(48) Robin, M. B.; Day, P. *Adv. Inorg. Chem. Radiochem.* **1967**, *10*, 247.